H Atom Branching Ratios from the Reactions of CH with C_2H_2, C_2H_4, C_2H_6, and *neo*-C_5H_{12} at Room Temperature and 25 Torr

Kenneth McKee, Mark A. Blitz, Kevin J. Hughes, Michael J. Pilling, Hai-Bo Qian, Andrew Taylor, and Paul W. Seakins*

School of Chemistry, University of Leeds, Leeds LS2 9JT, U.K.

Received: July 15, 2002; In Final Form: April 30, 2003

Branching ratios for H atom production from the reaction of CH($X^2\Pi$) with C_2H_2, C_2H_4, C_2H_6, and *neo*-C_5H_{12} have been measured relative to that from the CH + CH_4 reaction using laser-induced fluorescence at 121.56 nm (Lyman α). Assuming that the reaction with methane proceeds solely to the formation of H + C_2H_4, then the observed branching ratios are as follows: C_2H_2 1.05 ± 0.09, C_2H_4 1.09 ± 0.14, C_2H_6 0.14 ± 0.06, and *neo*-C_5H_{12} −0.10 ± 0.12 (errors refer to ±1σ). The results for the reaction of CH with acetylene and ethene are in good agreement with previous experimental and theoretical calculations. The yield of H atoms from the reaction of CH with ethane is consistent with a competition between C−H and C−C cleavage in an initially formed 1-propyl radical. The absence of H production for the reaction of CH with 2,2-dimethylpropane can be rationalized by the opening of isomerization pathways that lead to intermediates that dissociate only via C−C cleavage.

Introduction

The methylidene radical (CH) plays an important role in a variety of chemical environments, ranging from interstellar chemistry[1,2] through planetary atmospheres[3] to combustion chemistry.[4,5] The kinetics of CH removal are now well studied following extensive measurements by Lin and co-workers[6−9] and more recently by Smith and co-workers,[10,11] Taatjes and co-workers,[12−14] ourselves,[15−18] and others.[19−21] In general, CH reactions are characterized by fast barrierless insertion reactions forming an intermediate that rapidly decomposes to products, although there is debate as to the exact nature of the reaction mechanisms.[22−24] The absence of any pressure dependence in the removal kinetics of most reactions and the high rate coefficients show that stabilization and redissociation to form reagents are not competitive with dissociation of the intermediate to products.

A full understanding of the role of CH reactions is limited by our lack of knowledge of their product distributions. The high enthalpy of formation of the CH radical ($\Delta_f H$ = 595 kJ mol^{-1})[25] generally means that there are many thermodynamically accessible product channels. Determination of product branching ratios is vital not only for modeling the complex chemical systems that CH radicals participate in, but also in determining the mechanisms of CH reactions.

While a number of products have been observed from CH reactions, little quantitative data exist on the branching ratios. Hershberger and co-workers[26−28] have used tuneable IR diode laser spectroscopy to monitor the products of CH reactions; however, significant mechanistic interpretation is required because in some cases it is secondary products that are being observed rather than the direct products of the CH reaction. Dorthe and co-workers have used laser-induced fluorescence (LIF) to detect primary and secondary products from CH reactions in a fast-flow system,[29,30] but determination of absolute concentrations from LIF experiments is difficult.

In this paper, we report the use of LIF to detect the direct H atom product from a number of CH reactions.

$$CH + C_2H_2 \rightarrow C_3H_3 \rightarrow \text{products} \quad \text{(R1)}$$

$$CH + C_2H_4 \rightarrow C_3H_5 \rightarrow \text{products} \quad \text{(R2)}$$

$$CH + C_2H_6 \rightarrow 1\text{-}C_3H_7 \rightarrow CH_3 + C_2H_4 \quad \text{(R3a)}$$

$$\rightarrow H + C_3H_6 \quad \text{(R3b)}$$

$$CH + \textit{neo}\text{-}C_5H_{12} \rightarrow C_6H_{13} \rightarrow \text{products} \quad \text{(R4)}$$

Our approach has been to use a calibration reaction that only generates H, the reaction of CH with methane, to determine H atom branching yields. Identical concentrations of CH are generated with first methane and then the test reagent in excess. After one allows for background H production and the relative quenching efficiencies of methane and the test reagent, the ratio of H atom signals can be converted to a branching ratio.

For the reaction with acetylene, there are three theoretical studies[22,24,31] and one experimental study[32] with which to compare our results, all of which predict high H atom yields. The theoretical and experimental background for the other reactions is less comprehensive, but reactions 2 and 3 are expected to proceed via well-defined intermediates for which there are experimental data on their decomposition pathways.

Experimental Section

The reactions were studied using a conventional slow-flow laser flash photolysis apparatus[15−18] (25 Torr He, 295 K) with detection of the H atom product via Lyman α laser-induced fluorescence at 121.56 nm. A relatively low pressure was chosen to minimize the residence time of the gas mixtures within the cell allowing the replacement of several cell volumes between laser shots.

10.1021/jp021613w CCC: $25.00
Published on Web 07/08/2003

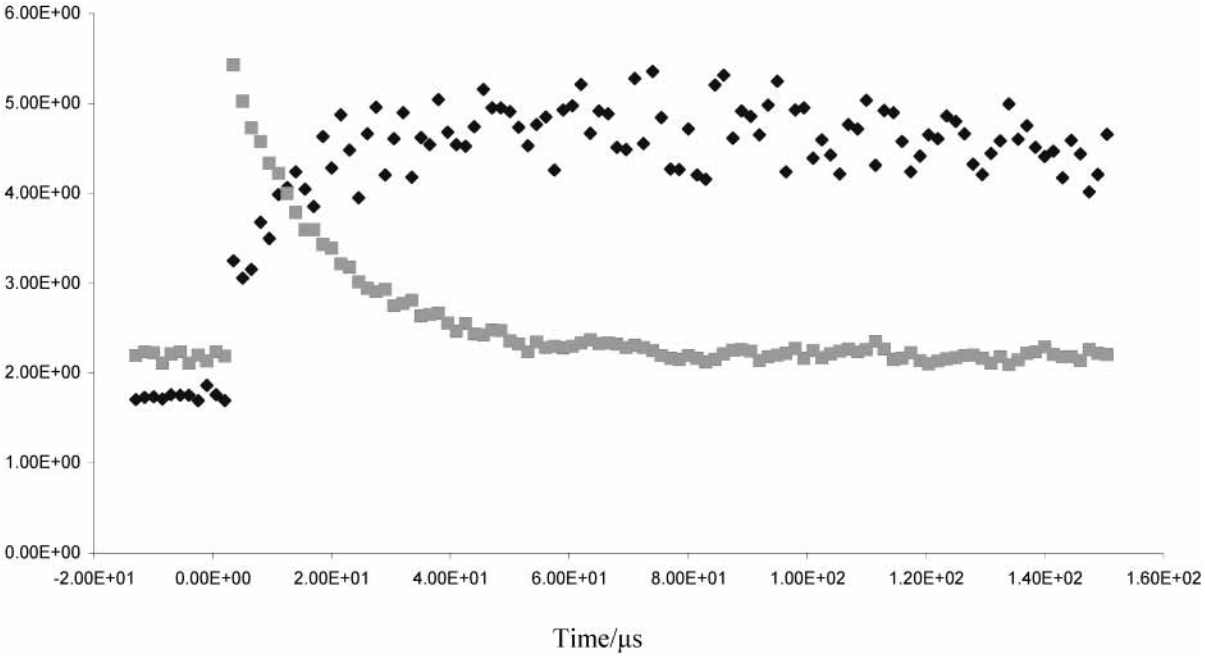

Figure 1. Kinetic trace showing the prompt production and subsequent growth of H atom signal and the decay of CH radicals from the reaction of CH with methane: $[CHBr_3] = 1.5 \times 10^{13}$ molecule cm^{-3}; $[CH_4] = 4.6 \times 10^{14}$ molecule cm^{-3}; 25 Torr He.

Lyman α was generated by frequency tripling 364.8 nm radiation from a dye laser (15−25 mJ pulse^{-1}, Lambda Physik FL2002, operating on *p*-terphenyl and pumped at 308 nm by a Questek excimer laser). The tripling was accomplished by focusing the 364.8 output into ∼30 Torr of krypton using a quartz 10 cm focal length lens.[33] Lyman α radiation was coupled into the reaction cell via a MgF_2 window and resonant radiation detected at right angles to both the photolysis and probe beams with a solar blind photomultiplier tube (Thorn-EMI 9423b).

CH radicals were generated by 248 nm photolysis of bromoform (∼200 mJ pulse^{-1}, unfocused radiation (2 cm^2) from Lambda Physik Lextra 50). The initial concentration of CH is difficult to calculate because of the multiphoton nature of the dissociation. We estimate $[CH]_0$ to be on the order of 10^{10} molecule cm^{-3}. Any (CH $A^2\Delta$, $B^2\Sigma$) rapidly relaxes back to the ground state.[15] We know from previous studies[15] that small (<10%) quantities of vibrationally excited CH are formed, which will contribute to the product spectrum. However, we would not expect that the relatively small increase in energy arising from vibrational excitation would have a significant effect on the product spectrum of a barrierless reaction. The major coproducts of the photolysis are thought to be $CHBr_2$, Br, and HBr.[34] The most likely fate of the dibromomethyl radical is radical recombination. Addition or abstraction reactions of bromine atoms are very slow under the experimental conditions and would be unlikely to generate H atoms as products. H atoms could be lost via reaction with HBr, but even assuming that 50% of the bromoform was photolyzed to HBr, the pseudo-first-order rate coefficient for H atom loss is only 45 s^{-1}.[35] A consistent first-order loss will have no effect on the ratio of H atoms at a fixed time delay after photolysis. CHBr is not thought to be a significant product of bromoform photolysis;[34] minor production of this radical is unlikely to interfere because the rate coefficients for CHBr reactions will be significantly lower than CH and Br will always be a more likely leaving group than H.

H atoms are also produced in the photolysis pulse. We account for photolytic H by removing CH via reaction with nitrogen. At room temperature, this reaction proceeds via complex formation and therefore without H atom production.

$$CH + N_2 + M \rightarrow HCN_2 + M \qquad (R5)$$

Although the reaction with bromoform should also remove CH without generating H, nitrogen was added so that CH was rapidly removed preventing H atom generation via CH recombination and ensuring that the kinetics of CH were similar for all types of experiments. The H atom signal recorded in the presence of N_2 corresponds to photolytic H (I_0).

Calibration is achieved via reaction with methane. The reaction is thought to proceed via CH insertion into methane giving an excited ethyl intermediate.[17,23]

$$CH + CH_4 \rightarrow C_2H_5 \rightarrow C_2H_4 + H \qquad (\Delta_r H = -251 \text{ kJ mol}^{-1})^{25} \quad (R6)$$

Of the other possible channels $CH_2 + CH_3$ is endothermic ($\Delta_r H = 18$ kJ mol^{-1})[25] and thus incompatible with the observed fast reaction rate ($k_{300} = 9.0 \times 10^{-11}$ cm^3 molecule^{-1} s^{-1})[18] and negative temperature dependence; the barrier to the thermodynamically accessible $C_2H_3 + H_2$ channel ($\Delta_r H = -221$ kJ mol^{-1})[25] is calculated to be too high and too constrained to compete with simple H atom elimination.[36] Fleurat-Lessard et al.[36] also measured the H atom yield from reaction 6 and found a 100% yield in line with their calculations.

An example of a kinetic trace with both the removal of CH and the production of H from the reaction of CH with methane is shown in Figure 1. The prompt production of H atoms from photolysis can clearly be seen, along with a growth in H atom signal corresponding to the decay of CH radicals.

The H atom signal recorded in the presence of CH_4 corresponds to photolytic H and the conversion of all the CH into H (I_{CH_4}). In the branching ratio experiments, the probe laser is fired at a fixed delay of 200 μs after the initial photolysis pulse; we do not record kinetic traces but rather fix the probe laser to measure the peak concentration of H atoms. Figure 2 shows a typical experimental trace with background (N_2) and calibration (CH_4) levels. In some experiments, ethene was used as the calibrant.

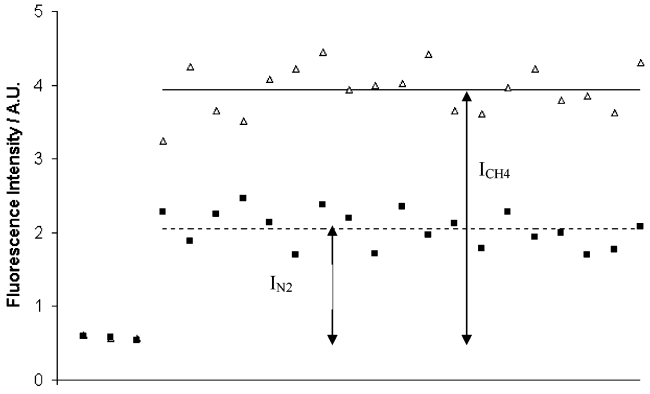

Figure 2. H atom signals recorded 200 μs after photolysis. Each point represents the average value of five laser pulses. Upper trace (diamonds) is the signal from a calibration mixture ($[CHBr_3] = 1.2 \times 10^{13}$ molecule cm^{-3}; $[CH_4] = 1.15 \times 10^{15}$ molecule cm^{-3}; 25 Torr He). The lower trace is with a nitrogen substrate to determine the photolytic H ($[CHBr_3] = 1.2 \times 10^{13}$ molecule cm^{-3}; $[N_2] = 3.67 \times 10^{17}$ molecule cm^{-3}; 25 Torr He).

Methane is then replaced with the test reagent, and the process is repeated (I_{TEST}). For all reactions, reagent concentrations were adjusted to give similar pseudo-first-order rate coefficients for removal of CH, and this value was large compared to loss of CH via reaction with bromoform (<10% of CH lost via reaction with bromoform for CH_4/N_2 and <5% for all other gases). The fraction of CH reacting with the test gas was determined by observing the pseudo-first-order rate coefficients for CH removal in the presence and absence of the test or calibrant gas.

The delay of 200 μs between photolysis and probe pulses was chosen to ensure all CH had reacted but before any possible secondary reactions can have generated H. H atom decay profiles taken over longer times exhibited purely diffusional behavior suggesting that there is no significant generation of H atoms by secondary reactions. Diffusional loss within the first 200 μs was minimal (<2%), and assuming that diffusional loss can be approximated to a first-order process and that it remains constant for experiments (a plausible assumption considering all studies were carried out at a constant bath gas pressure), it will have no effect on the ratios of H atoms concentrations. For the unsaturated hydrocarbons, addition of H atoms becomes a possible loss mechanism. Due to the high rate coefficients for CH reactions with ethene and acetylene, only low concentrations of unsaturated hydrocarbons are required to ensure that CH is primarily removed by reaction with the test gas. Therefore the pseudo-first-order rate coefficients for loss of H atoms are kept at a low level (<200 s^{-1}) and a corresponding maximum 4% loss of H atoms. No significant change in was observed in the branching ratio as the probe delay was varied between 100 and 300 μs. For the saturated hydrocarbons, H atom abstraction is too slow at room temperature to be a significant loss process.

Determination of the H atom yield requires a correction factor (C) for the fluorescence signal to account for quenching or absorbance by the various reagent gases. Figure 3 shows an example of a calibration plots obtained by monitoring the H atom signal at a constant H concentration, generated from H_2S photolysis (~10 mTorr), at various reagent concentrations. Absorbance cross sections calculated showed good agreement with literature values.[25] Quenching cross sections for the excited 2P state were consistent with deactivation of the excited state after each collision of the quenching molecule.[37]

The branching ratio, α, is calculated from

$$\alpha = \frac{C_{TEST} I_{TEST} - C_{N_2} I_{N_2}}{C_{CAL} I_{CAL} - C_{N_2} I_{N_2}} \qquad \text{(E1)}$$

where I_X is the raw H atom fluorescence signal for the test, calibrant (CH_4 or C_2H_4), or nitrogen and C is the appropriate correction factor to account for the reduction in H atom fluorescence due to the particular gas. Determination of the branching ratios was carried out by comparing test signals to calibrant signals and then calibrant-to-nitrogen ratios. The equation can be rearranged to give the branching ratio in terms of the ratios.

$$\alpha = \frac{\frac{C_{TEST}}{C_{CAL}}\frac{I_{TEST}}{I_{CAL}} - \frac{C_{N_2}}{C_{CAL}}\frac{I_{N_2}}{I_{CAL}}}{1 - \frac{C_{N_2}}{C_{CAL}}\frac{I_{N_2}}{I_{CAL}}} \qquad \text{(E2)}$$

The raw experimental ratios, correction factors, and calculated values for each test gas are presented in Table 1.

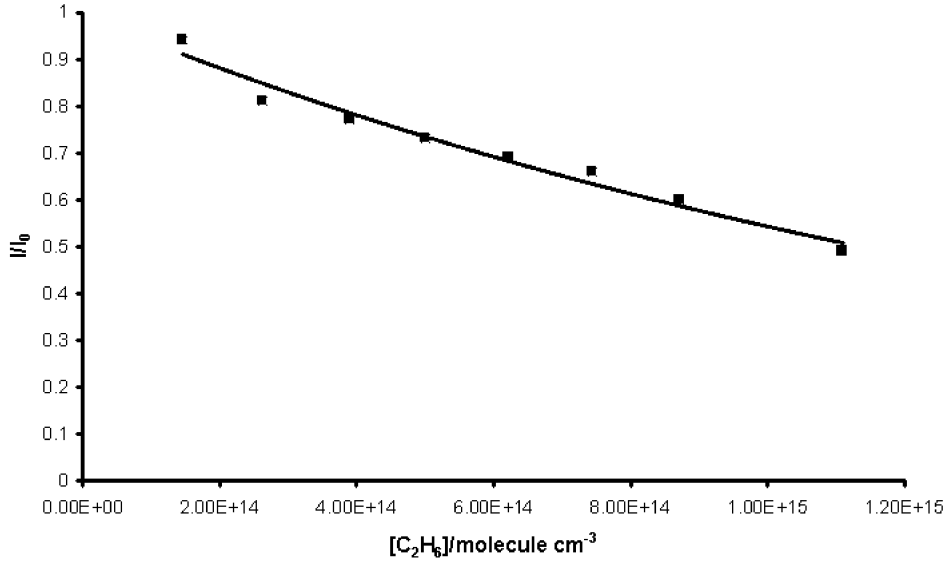

Figure 3. Calibration curve for ethane. Solid line is a fit to $(I/I_0) = e^{\sigma c l}$, where the path length, l, was 21 cm. The measured value for the cross section is $(2.97 \pm 0.11) \times 10^{-17}$ cm^2.

TABLE 1: Experimental Conditions, Signal Ratios, and Branching Ratios

reaction	[test reagent], molecule cm^{-3}	I_{TEST}/I_{CAL}	I_{N_2}/I_{CAL}	C_{TEST}	H atom yield	H atom yield corrected for CH loss
$CH + C_2H_2$	3.8×10^{14}	0.88 ± 0.06	0.45 ± 0.03^a	1.89	1.14	1.05 ± 0.09
$CH + C_2H_4$	2.9×10^{14}	1.43 ± 0.06	0.45 ± 0.03^a	1.20	1.24	1.09 ± 0.14
$CH + C_2H_6$	5.6×10^{14}	0.83 ± 0.02	0.45 ± 0.03^a	1.52	0.20	0.18 ± 0.06
$CH + C_2H_6$	5.6×10^{14}	0.56 ± 0.07	0.34 ± 0.03^b	1.52	0.12	0.10 ± 0.07
$CH + neo\text{-}C_5H_{12}$	8.1×10^{14}	0.29 ± 0.03	0.34 ± 0.03^b	2.13	−0.15	-0.10 ± 0.12

[a] CH_4 as calibrant. $[CH_4] = 1.32 \times 10^{15}$ molecule cm^{-3}; $C_{CH_4} = 1.58 \pm 0.04$. [b] C_2H_4 as calibrant. $[C_2H_4] = 8.14 \times 10^{14}$ molecule cm^{-3}. $[N_2] = 3.4 \times 10^{17}$ molecule cm^{-3}, $C_{N_2} = 2.20 \pm 0.05$. $[CHBr_3] = 1.5 \times 10^{13}$ molecule cm^{-3}. Total pressure = 25 Torr with He as added bath gas.

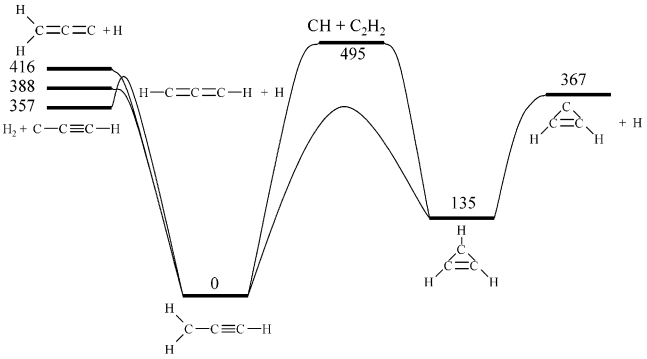

Figure 4. Simplified schematic potential energy diagram for the reaction of CH with C_2H_2 based on the calculations of Vereecken et al.[38] Values are in kJ mol^{-1}.

For this initial study, we have operated at constant temperature and pressure. Theoretical calculations[22] suggest little variation in the product yields for the chosen reactions over the temperature and pressure ranges accessible with the current apparatus. Therefore, for this particular set of reactions, it was not considered worthwhile to determine correction factors at variety of conditions, although they may need to be determined in future studies.

Results and Discussion

The results of the experimental determinations are presented in Table 1. The branching ratios are weighted means of 8−10 separate determinations. The error limits correspond to the standard error of the mean at the 1σ level. Within experimental error, the H atom yield for the reaction with acetylene and ethene is unity; that for 2,2-dimethylpropane (*neo*-pentane) is zero. There have been no previous experimental observations of H atom yields, but for acetylene, there have been some theoretical calculations and an experimental determination of C_3H_2 and C_3H production. The results for each of the reagents are discussed in the following sections.

Acetylene. Vereecken, Pierloot and Peeters[38] have calculated a very detailed potential energy surface (PES) for reaction 1 (DFT and CASPT2 characterization), shown in simplified form in Figure 4. There are three possible initial steps with CH adding across the triple bond to form a cyclic C_3H_3 intermediate, inserting into a CH bond, or adding to a carbon. The calculations predict that insertion and cycloaddition are comparable with insignificant terminal addition (<10%). The experimental observation by Thiesemann et al.[14] of no kinetic isotope effect upon deuteration of acetylene suggests that addition may be the more dominant initial step. Master equation calculations indicate that, as expected for such exothermic reactions, stabilization will not compete with dissociation for any of the adducts.[22]

The H_2CCCH (2-propynyl or propargyl) isomer is formed via insertion and is also accessible from cycloprop-2-enyl isomer (formed from cycloaddition). The stability of the propargyl radical means that it is the dominant C_3H_3 isomer formed, despite the predicted comparability of the rates of the two entrance channels.[38] The primary dissociation mechanism from H_2CCCH is calculated to be H atom elimination to form triplet HCCCH. The alternative H_2 elimination process is calculated to contribute less than 3% to the reaction under our experimental conditions.[22] Formation of the cyclic C_3H_3 also leads to H atom formation and overall, under our experimental conditions, the combined ab initio and master equation calculations predict 97% H atom formation,[22] in good agreement with the current experimental results.

The calculations and our experimental results give low yields of HCCC + H_2 products, despite the greater exothermicity of this channel. Vereecken and Peeters[22] rationalize their prediction of minimal H_2 production by comparing the tight transition state for HCCC + H_2 formation (comparable in energy to triplet HCCCH + H) with the very loose variational transition state for triplet HCCCH + H and hence a much greater sum of states for the latter channel.

Nguyen et al.[31] also used the PES calculated by Vereecken et al.[38] to model reaction 1 using Rice−Ramsperger−Kassel−Marcus (RRKM) calculations under collision-free conditions. As might be expected, the results are compatible with the calculations carried out by Vereecken and Peeters.[22]

Boullart et al.[32] have measured the branching ratio of reaction 1 at 2 Torr and 600 K. Their results, 85^{+9}_{-15}% C_3H_2 + H and 15^{+15}_{-9}% C_3H + H_2, are in agreement with the calculation,[22] although with a higher H_2 yield. According to the ab initio/master equation calculations,[22] the H atom branching ratio should be very similar for the experimental conditions used in both this work and that of Boullart et al.,[32] and within error, the two experimental determinations are in agreement. In their experiment, which involved observation of steady-state radical concentrations following the O + C_2H_2 reaction (producing CH_2 + CO followed by CH_2 + H → CH + H_2), Boullart et al. were able to directly observe C_3H, so unless there was another mechanism for C_3H generation under their experimental conditions other than reaction 1, production of H must be less than unity.

An earlier, less-detailed ab initio calculation[24] (CASSCF-ICCI) gives a similar H atom yield but predicts that the coproduct is the H_2CCC biradical. If this mechanism is correct, then the product H atom would originate solely from the acetylene reagent. Conversely, HCCCH formation would be expected to occur via elimination from the CH_2 fragment of the H_2CCCH intermediate, and hence, ∼50% of the H will be from the CH and 50% from acetylene. Future experiments comparing D yields from combinations of isotope reactions such as CH + C_2D_2 and CD + C_2H_2 may therefore shed some light on the nature of the coproducts from reaction 1.

Ethene. The kinetics of the methylidene and ethene reaction have been studied by three groups.[3,12,39] All measurements show

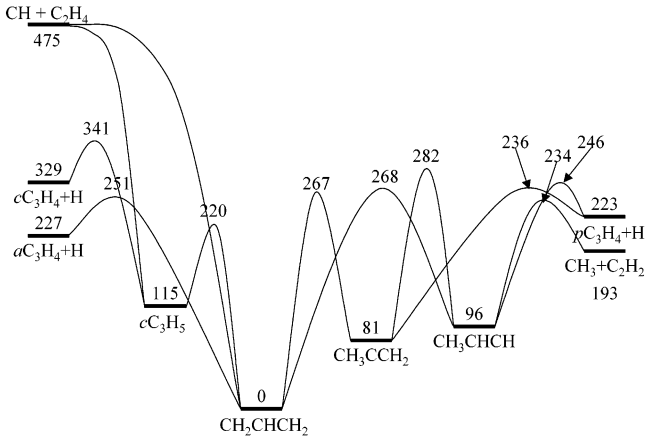

Figure 5. Schematic potential energy diagram for the reaction of CH with C_2H_4. Values for the intermediates and transition states are based on the calculations of Davis et al.[42] and Deyerl et al.[43]

a negative temperature dependence and are reasonably consistent in their room-temperature measurements ($(2.9-4.2) \times 10^{-10}$ cm^3 $molecule^{-1}$ s^{-1}). A number of theoretical calculations exist on the initial step of the CH + C_2H_4 reaction.[12,40,41] As for the reaction of CH with acetylene, the reaction with ethene can proceed via either insertion or addition. An early calculation at the CISDQ/6-31G//ROHF/6-31G level[40] predicted a barrier for insertion suggesting that the addition reaction is dominant; however, later, higher-level calculations (QCISD(T)/6-311++G-(3df,2pd),[12] MP2/6-31G(d,p)[41]) show no barrier for the insertion reaction. Quantum chemical calculations by Thiesemann et al.[12] suggest that the initial step of the reaction is dominated by addition and the small isotope effect upon ethene deuteration observed by these workers seems to support addition being the dominant mechanism.

Addition leads to cyclopropyl (cC_3H_5) and insertion to allyl (CH_2CHCH_2), and the two intermediates can be interconverted by ring cleavage/cycloaddition. Figure 5 shows a schematic potential energy surface based on the calculations of Davies et al.[42] for the production of allene, methylpropyne, and CH_3 + C_2H_4 (G2(B3LYP)) and Deyerl et al.[43] (MP4/6-31G* and single-point CCSD(T) coupled cluster calculations for the determination of activation barriers) for the production of cyclopropene not considered by Davies et al. Two of the H atom product channels (H + cyclopropene, [cC_3H_4], and H + allene, [aC_3H_4]) are accessible directly from allyl and cyclopropyl; the formation of the other potential products (CH_3 + C_2H_2 and H + propyne, [pC_3H_4]) requires isomerization to the 1-propenyl (CH_3CHCH) and 2-propenyl radicals (CH_3CCH_2), respectively.

The fate of any initially formed cyclopropyl is likely to be conversion to allyl. Deyerl et al. calculated a dissociation barrier to form cyclopropene that is over 84 kJ mol^{-1} higher than the barrier for C−C cleavage to form allyl and significantly higher than barriers to other intermediates and products accessible from allyl. Because of the much lower energy of allyl compared to cC_3H_5, allyl will be the dominant C_3H_5 isomer and product formation will be dominated by reactions originating from the allyl radical, and hence, the yield of cyclopropene is expected to be small.

Production of CH_3 + C_2H_2, and hence a less than 100% yield of H atoms, arises from isomerization to the 1-propenyl radical from allyl either by two 1,2 H shifts or via a single 1,3 shift. The latter mechanism seems more plausible considering the high energy barrier for the second 1,2 isomerization from 2-propenyl compared to H + *a* and pC_3H_4 formation. A lower limit for the H atom branching ratio (BR_H) can be obtained by comparing the microcanonical rate coefficients ($k(E)$'s) for dissociation to H atom channels (H + aC_3H_4 from allyl and H + aC_3H_4 and H + pC_3H_4 from 2-propenyl) with that for the 1,3 isomerization to 1-propenyl products.

$$BR_H = \frac{k(E)_{H+aC_3H_4} + k(E)_{1,2shft}}{k(E)_{H+aC_3H_4} + k(E)_{1,2shft} + k(E)_{1,3shft}} \qquad (E3)$$

This expression presumes that dissociation of 1- and 2-propenyl occurs with unit efficiency on formation and neglects regeneration of allyl by reverse isomerization and therefore provides a lower limit for the branching ration. From RRKM theory,[44]

$$k(E) = \frac{W(E^+)}{h\rho(E^*)} \qquad (E4)$$

where $W(E^+)$ is the sum of vibrational states of the particular transition state with available energy E^+ and $\rho(E^*)$ is the density of states of the allyl radical at total energy E^* and will be common to each of the $k(E)$ terms.

Davis et al.[42] have calculated the barrier heights (G2(B3LYP)) and the vibrational frequencies of the associated transition states at the B3-PW91/6-31G(d,p) level. These have been utilized in a state counting program based on the Beyer−Swinehart algorithm to calculate $W(E)$ for each of the possible initial transition states leading from allyl to products. The calculations predict H production of 98% ± 1% in good agreement with our experimental determination. Error limits on the calculation are based on variations of 1 kcal mol^{-1} in the energies of the transition states and the differences in the resulting values of $W(E)$. A similar calculation suggests that over 94% of the reaction yields allene as the C_3H_4 product.

Support for the calculated distribution of C_3H_4 products comes from the work of Fischer and Chen[45] who examined the yields of H and D following the 248 nm photolysis of CD_2CHCD_2. Internal conversion from the initially formed C state releases ~481 kJ mol^{-1} of internal energy into the ground-state allyl radical, very similar to the 472 kJ mol^{-1} of energy released on chemical activation from the CH + C_2H_4 reaction. The observed H/D ratio of ~10:1 is consistent with allene being the primary product; cyclopropene would result in the loss of D, and propyne production would scramble H and D.

However, Fischer and Chen were only able to detect H or D products. Stranges et al.[46] have also studied the 248 nm photodissociation of allyl; their time-of-flight mass spectrometry detection allows observation of the molecular fragments. Energy-resolved C_3H_4 mass spectra confirm the absence of a significant cyclopropene yield, but because of the similar energies of allene and propyne, these studies cannot identify whether allene or propyne is the dominant C_3H_4 product.

More interestingly, Stranges et al. observed a significant, 16%, CH_3 + C_2H_2 production with 248 nm photolysis, in contrast to our observations. They supported their results with RRKM calculations from an empirical energy surface with CH_3 + C_2H_2 production from allyl via a direct mechanism not present in the surface of Davies et al., as well as from the 1,3 migration to 1-propenyl. The calculations predicted 27% and 31% yields of CH_3 + C_2H_2 at 248 and 351 nm photolysis, respectively. The barriers used for the isomerizations were very much lower than those calculated more recently by Davies et al., and the prediction of enhanced CH_3 + C_2H_2 production at longer photolysis wavelengths was not matched by experimental observation where the CH_3 + C_2H_2 channel was below the experimental detection limit for 351 nm photolysis of allyl.

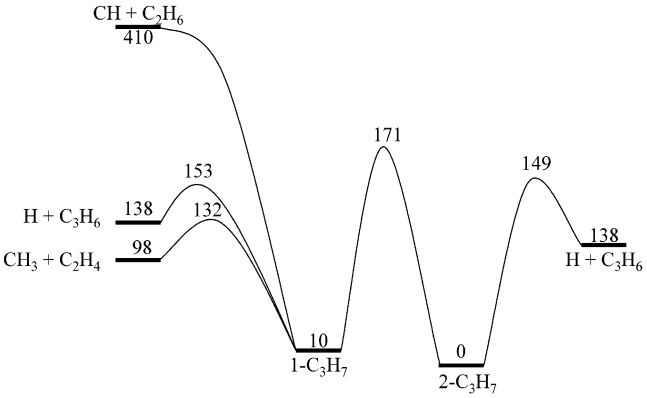

Figure 6. Schematic potential energy diagram for the reaction of CH with C_2H_6. Values for the transition states are taken from Yamauchi et al.[48]

TABLE 2: Preexponential Factors and Threshold Energies[48] for 1-Propyl Reactions

reaction	*A* factor (s^{-1})	E_0 (kJ mol^{-1}),	available energy at transition state, E^+ (kJ mol^{-1})[a]
1-C_3H_7 → CH_3 + C_2H_4	1.8×10^{14}	122	278
1-C_3H_7 → C_3H_6 + H	1.4×10^{14}	143	257
1-C_3H_7 → 2-C_3H_7	1.6×10^{13}	161	239

[a] Chemical activation from reaction 3 delivers 400 kJ mol^{-1} of energy, E^*, to the 1-propyl intermediate. $E^+ = E^* - E_0$.

The basic structure of the PES calculated by Davies et al. has recently been confirmed by observations on the decomposition of allyl formed following the 193 nm photolysis of C_3H_5-Cl. In this study, Morton et al.[47] were also unable to observe any CH_3 + C_2H_2 products.

Ethane. The initial step in this reaction is thought to be CH insertion into the C−H bonds of ethane forming the 1-propyl intermediate. Two possible dissociation channels are open; formation of H + propene and CH_3 + ethene, as well as isomerization to the 2-propyl radical (from which the only decomposition pathway is H + propene formation). A schematic of the potential energy diagram for reactions following the formation of 1-propyl is shown in Figure 6. An estimate of the product branching ratios can be made from the data on alkyl radical decompositions collated recently by Yamauchi et al.[48] and summarized in Table 2.

Fragmentation of the C−C bond has the lower activation energy of the 1-propyl decomposition routes; the calculated *A* factors are comparable. Isomerization to 2-propyl is likely to be uncompetitive with dissociation because it has an activation barrier still higher than either dissociation pathway and a small *A* factor due to the constrained transition state for the 1,2 H atom shift.

Product branching ratios can be calculated from the energy-dependent rate coefficients ($k(E)$) for the two dissociation channels and isomerization. Data on the transition states are not available for these reactions, but $k(E)$ can be obtained from Arrhenius representations of the 1-propyl reactions via an inverse Laplace transformation[44] such that

$$k(E) = \frac{A\rho_{1-\text{propyl}}(E^+)}{\rho_{1-\text{propyl}}(E^*)} \qquad \text{(E5)}$$

where $\rho_{1-\text{propyl}}(E^+)$ is the density of states of the 1-propyl radical with the energy available at the transition state for a particular pathway and $\rho_{1-\text{propyl}}(E^*)$ is the density of states of the 1-propyl

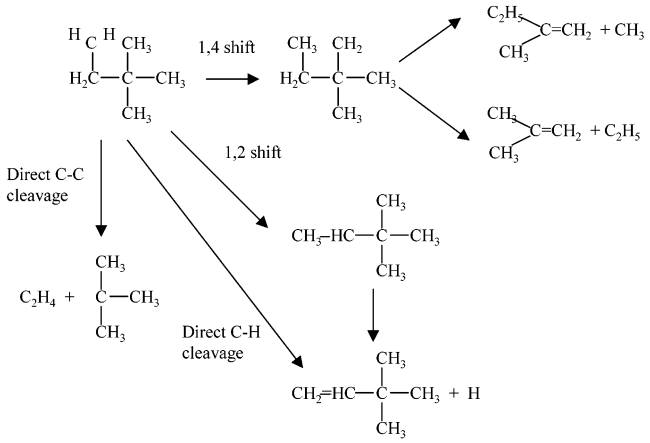

Figure 7. Reactive pathways in the CH + *neo*-C_5H_{12} reaction.

at the total energy. Vibrational densities of states for 1-propyl were calculated using the Beyer−Swinehart algorithm with the 1-propyl frequencies given in ref 49. The branching ratio for H atom formation, BR_H, becomes

$$BR_H = \frac{A_{H+C_3H_6}\rho_{1-\text{propyl}}(E^+) + A_{\text{isomerization}}\rho_{1-\text{propyl}}(E^+)}{A_{CH_3+C_2H_4}\rho_{1-\text{propyl}}(E^+) + A_{H+C_3H_6}\rho_{1-\text{propyl}}(E^+) + A_{\text{isomerization}}\rho_{1-\text{propyl}}(E^+)} \qquad \text{(E6)}$$

Using eq 6, we calculate the branching ratio for H atom formation to be 23%, comparable with the experimental determination, 14% ± 6%, obtained by averaging the independent determinations made using methane and ethane as calibrants. Simultaneously increasing the barrier for C−H dissociation and decreasing the barrier for C−C dissociation by 1 kcal or vice versa produces H atom branching ratios of 17% and 31%, respectively. The branching ratio to isomerization is <1% confirming our assumption that formation of the 2-propyl radical plays little role in the reaction.

An alternative mechanism for H atom formation would be the insertion of CH into the C−C bond of ethane forming the 2-propyl radical directly. Our preliminary calculations suggest that one does not need to invoke an additional pathway to account for the observed H atom yield. Studies on the H/D yields are unlikely to yield experimental evidence for the existence of such an insertion mechanism (both C−H and C−C insertions can give similar products). Evidence is more likely to come from kinetic isotope effects; deuteration of methane, where on C−H insertion is possible, produces a considerable isotope effect;[14,18] one would expect a kinetic isotope effect of similar magnitude with ethane deuteration if the C−H insertion dominates.

Qualitative support for significant H atom production comes from the work of Min et al.[50] and Wang et al.[51] who have looked at the H/D atom kinetic energy spectra following photolysis of 1-propyl radicals at 193−248 nm, but their studies did not include a determination of an absolute branching ratio.

2,2-Dimethylpropane. Within experimental error, the H atom yield from this reaction is zero. The errors are quite large because we are subtracting numbers of very similar magnitude (I_{TEST} and I_0) when determining the branching ratio. Insertion into the C−H bonds of 2,2-dimethylpropane yields the CH_2-$CH_2C(CH_3)_3$ intermediate shown in Figure 7.

As for ethane, two possible dissociation pathways exist with H atom elimination giving H + 3,3-dimethylbut-1-ene and C−C fragmentation yielding ethene + *tert*-butyl. If these were the

only possible reaction pathways, then by analogy with ethane, we would still expect some H atom formation. However, for this reaction, 1,4 isomerizations are also possible and the low energy barriers (~90 kJ mol^{-1})[48] for this process make it competitive with direct dissociation. The product of this isomerization has no hydrogen atoms α to the radical site and is likely to dissociate via C−C cleavage. Calculations on the C_5H_{11} system will be required to verify whether this proposed explanation is valid.

Conclusions

A technique for the measurement of the branching ratios of H atoms has been demonstrated for CH radicals. The general principle can be applied to a variety of other reaction systems as long as an appropriate calibration reaction is available. Good agreement with theory and experiment has been obtained for the reactions of CH with acetylene and ethene, although our results do not agree with one study on allyl decomposition.[46] For the reactions with ethane and 2,2-dimethylpropane, there are no previous experiments or calculations with which to compare our results, but our yield of H atom from ethane is in agreement with a preliminary calculation based on inverse Laplace transformation of Arrhenius parameters for the component reactions. More detailed calculations on this reaction are planned for the near future. No H atoms were detected from the reaction of CH with 2,2-dimethylpropane, and this observation can be rationalized by the presence of competitive 1,4 isomerizations leading to a radical that can dissociate only via C−C cleavage.

Acknowledgment. The authors acknowledge EPSRC (Grant GR/N00913) for funding and the referees for a number of constructive comments.

References and Notes

(1) Amin, M. Y.; El Nawawy, M. S. *Earth, Moon, Planets* **1997**, *75*, 25.
(2) Brownsword, R. A.; Sims, I. R.; Smith, I. W. M. *Astrophys. J.* **1997**, *485*, 195.
(3) Canosa, A.; Sims, I. R.; Travers, D.; Smith, I. W. M.; Rowe, B. R. *Astron. Astrophys.* **1997**, *323*, 644.
(4) Miller, J. A.; Bowman, C. T. *Prog. Energy Combust. Sci* **1989**, *15*, 287.
(5) Miller, J. A.; Kee, R. J.; Westbrook, C. *Annu. Rev. Phys. Chem.* **1990**, *41*, 345.
(6) Berman, M. R.; Lin, M. C. *J. Chem. Phys* **1984**, *81*, 5743.
(7) Lichtin, D. A.; Berman, M. R.; Lin, M. C. *Chem. Phys. Lett*. **1984**, *108*, 18.
(8) Berman, M. R.; Lin, M. C. *Chem. Phys* **1983**, *82*, 435.
(9) Berman, M. R.; Lin, M. C. *J. Phys. Chem*. **1983**, *87*, 3933.
(10) Brownsword, R. A.; Canosa, A.; Rowe, B. R.; Sims, I. R.; Smith, I. W. M.; Stewart, D. W. A.; Symonds, A. C.; Travers, D. *J. Chem. Phys*. **1997**, *106*, 7662.
(11) Herbert, L. B.; Sims, I. R.; Smith, I. W. M.; Stewart, D. W. A.; Symonds, A. C.; Canosa, A.; Rowe, B. R. *J. Phys. Chem.* **1996**, *100*, 14928.
(12) Thiesemann, H.; Clifford, E. P.; Taatjes, C. A. *J. Phys. Chem. A* **2001**, *105*, 5393.
(13) Taatjes, C. A. *J. Chem. Phys*. **1997**, *107*, 10829.
(14) Thiesemann, H.; MacNamara, J.; Taatjes, C. A. *J. Phys. Chem. A* **1997**, *101*, 1881.
(15) Blitz, M. A.; Pesa, M.; Pilling, M. J.; Seakins, P. W. *Chem. Phys. Lett*. **2000**, *322*, 280.
(16) Johnson, D. G.; Blitz, M. A.; Seakins, P. W. *Phys. Chem. Chem. Phys.* **2000**, *2*, 2549.
(17) Blitz, M. A.; Pesa, M.; Pilling, M. J.; Seakins, P. W. *J. Phys. Chem. A* **1999**, *103*, 5699.
(18) Blitz, M. A.; Johnson, D. G.; Pesa, M.; Pilling, M. J.; Robertson, S. H.; Seakins, P. W. *J. Chem. Soc., Faraday Trans.* **1997**, *93*, 1473.
(19) Anderson, S. M.; Freedman, A.; Kolb, C. E. *J. Phys. Chem.* **1987**, *91*, 6272.
(20) Becker, K. H.; Engelhardt, B.; Wiesen, P.; Bayes, K. D. *Chem. Phys. Lett*. **1989**, *154*, 342.
(21) Bergeat, A.; Calvo, T.; Caralp, F.; Fillion, J.-H. Dorthe, G.; Loison, J.-C. *Faraday Discuss*. **2001**, *119*, 67.
(22) Vereecken, L.; Peeters, J. *J. Phys. Chem. A* **1999**, *103*, 5523.
(23) Taatjes, C. A.; Klippenstein, S. J. *J. Phys. Chem. A* **2001**, *105*, 8567.
(24) Guadagnini, R.; Schatz, G. C.; Walch, S. P. *J. Phys. Chem. A* **1998**, *102*, 5857.
(25) *CRC Handbook of Chemistry and Physics*, 76th ed.; CRC Press: Boca Raton, FL, 1995. Okabe, H. *Photochemistry*; J. Wiley: New York, 1978.
(26) Rim, K. T.; Hershberger, J. F. *J. Phys. Chem. A* **1998**, *102*, 4592.
(27) Hovda, N.; Hershberger, J. F. *Chem. Phys. Lett.* **1997**, *280*, 145.
(28) Lambrecht, R. K.; Hershberger, J. F. *J. Phys. Chem*. **1994**, *98*, 8406.
(29) Bergeat, A.; Calvo, T.; Dorthe, G.; Loison, J.-C. *J. Phys. Chem. A* **1999**, *103*, 6360.
(30) Bergeat, A.; Calvo, T.; Daugey, N.; Loison, J.-C.; Dorthe, G. *J. Phys. Chem. A* **1998**, *102*, 8124.
(31) Nguyen, T. L.; Mebel, A. M.; Lin, S. H.; Kaiser, R. I. *J. Phys. Chem. A* **2001**, *105*, 11549.
(32) Boullart, W.; Devriendt, T.; Borms, R.; Peeters, J. *J. Phys. Chem*. **1996**, *100*, 998.
(33) Morley, G. P.; Lambert, I. R.; Ashfold, M. N. R.; Rosser, K. N. *J. Chem. Phys*. **1992**, *97*, 3157.
(34) McGivern, W. S.; Shorkhabi, O.; Suits, A. G.; Derecskei-Kovacs, A.; North, S. W. *J. Phys. Chem. A* **2000**, *104*, 10085.
(35) Seakins, P. W.; Pilling, M. J. *J. Phys. Chem.* **1991**, *95*, 9878.
(36) Fleurat-Lesard, P.; Rayez, J.-C.; Bergeat, A.; Loison, J.-C. *Chem. Phys.* **2002**, *279*, 87.
(37) McKee, K.; Blitz, M. A.; Pilling, M. J.; Seakins P. W., manuscript in preparation.
(38) Vereecken, L.; Pierloot, K.; Peeters, J. *J. Chem. Phys*. **1998**, *108*, 1068.
(39) Berman, M. R.; Fleming, J. W.; Harvey, A. B.; Lin, M. C. *Chem. Phys.* **1982**, *73*, 27.
(40) Gosavi, R. K.; Safarik, I.; Strausz, O. P. *Can. J. Chem.* **1985**, *63*, 1689.
(41) Wang, Z.-X.; Huang, M.-B. *Chem. Phys. Lett.* **1998**, *291*, 381.
(42) Davis, S. G.; Law, C. K.; Wang, H. *J. Phys. Chem. A* **1999**, *103*, 5889.
(43) Deyerl, H.-J.; Fischer, I.; Chen, P. *J. Chem. Phys* **1999**, *110*, 1450.
(44) Holbrook, K. A.; Pilling, M. J.; Robertson, S. H. *Unimolecular Reactions*; Wiley: Chichester, U.K., 1996.
(45) Fischer, I.; Chen, P. *J. Phys. Chem. A* **2002**, *106*, 4291.
(46) Stranges, D.; Stemmler, M.; Yang, X.; Chesko, J. D.; Suits, A. G.; Lee, Y. T. *J. Chem. Phys* **1998**, *109*, 5372.
(47) Morton, M.; Butler, L. J.; Stephenson, T. A.; Qi, F. *J. Chem. Phys* **2002**, *116*, 2763.
(48) Yamauchi, N.; Miyoshi, A.; Kosaka, K.; Koshi, M.; Matsui, H. *J. Phys. Chem. A* **1999**, *103*, 2723.
(49) Bencsura, A.; Knyazev, V.; Xing, S.-B.; Slagle, I. R.; Gutman, D. *Int. Symp. Combust.* **1992**, *24*, 629.
(50) Min, Z.; Quandt, R.; Bersohn, R. *Chem. Phys. Lett*. **1998**, *296*, 372.
(51) Wang, Z. G.; Matthews, M. G.; Koplitz, B. *J. Phys. Chem*. **1995**, *99*, 6913.